Demethylation of the *RORC2* and *IL17A* in Human CD4$^+$ T Lymphocytes Defines Th17 Origin of Nonclassic Th1 Cells

Alessio Mazzoni,[*,†,‡,§,1] Veronica Santarlasci,[*,†,¶,1] Laura Maggi,[*,†,¶] Manuela Capone,[*,†] Maria Caterina Rossi,[*,†] Valentina Querci,[*,†] Raffaele De Palma,[‡,§] Hyun-Dong Chang,[‖] Andreas Thiel,[#] Rolando Cimaz,[**] Francesco Liotta,[*,†,††] Lorenzo Cosmi,[*,†,††] Enrico Maggi,[*,†,††] Andreas Radbruch,[‖] Sergio Romagnani,[*,†] Jun Dong,[‖,2] and Francesco Annunziato[*,†,¶,2]

Th17-derived Th1 lymphocytes, termed nonclassic, differ from classic Th1 cells because of the presence of retinoic acid orphan receptor (ROR)C2 and the surface expression of CD161 and CCR6. We demonstrate in this article that nonclassic Th1 cells, like Th17 cells, have a marked *RORC2* and *IL17A* demethylation, whereas classic Th1 cells exhibit a complete methylation of these genes. The analysis of *RORC2* DNA methylation in the CD4$^+$CD161$^+$ and CD4$^+$CD161$^-$ naive Th subsets from umbilical cord blood surprisingly revealed comparable hypermethylation levels. PCR analysis at the single-cell level revealed that *RORC2* mRNA was expressed by none of the CD4$^+$CD161$^-$ and present only in a minority of CD4$^+$CD161$^+$ naive Th cells. These findings provide two important novel observations on the physiology of human Th17 cells: 1) they confirm at the epigenetic level the origin of nonclassic Th1 cells from Th17 cells, also identifying in the *RORC2* and *IL17A* methylation status a novel tool for their distinction from classic Th1 cells, and 2) they demonstrate that RORC2-expressing cells are only a minority in the subset of CD4$^+$CD161$^+$ naive Th cells, which are known to contain all Th17 cell precursors. ***The Journal of Immunology*, 2015, 194: 3116–3126.**

Activated CD4$^+$ T cells can be divided into functionally distinct subsets on the basis of their cytokine production and their specific transcription factor expression: Th1 secrete IFN-γ, express the transcription factor T-bet (T-box expressed in T cells, *TBX21*), and protect the host against intracellular infections; Th2 cells secrete IL-4, IL-5, and IL-13, express the transcription factor GATA-3, and mediate host defense against helminths; and Th17 cells, which selectively produce IL-17A, express the transcription factor retinoic acid orphan receptor (ROR)C2 and are critical for the host defense against extracellular pathogens (1–4). Moreover, a subset of human IL-17A–producing CD4$^+$ T cells was found also to produce IFN-γ (Th17/Th1), and both Th17 and Th17/Th1 cells exhibited plasticity toward the Th1 profile when cultured in the presence of IL-12 (4). Similar findings were then also reported in some murine models (5–7), suggesting that both human and murine Th17 cells probably represent a transient phenotype (8). In a previous study, we also showed that virtually all human memory Th17 cells are contained within the CD161$^+$ fraction of both circulating and tissue-infiltrating CD4$^+$ T cells, and originate from CD161$^+$ precursors present in umbilical cord blood (UCB) and newborn thymus (9), a finding that has not been reported in mice. In humans, Th1 cells that derive from the shifting of Th17 cells were defined as nonclassic Th1 cells (8, 10) because they express RORC2, CD161, and CCR6, as do Th17 cells (9–11).

Tissue- and cell-specific transcriptional regulatory programs are acquired during various stages of cellular differentiation and must persist into the cellular progeny to maintain the specialized functions of the cells in a particular tissue. Covalent modifications to histones and DNA, referred to as epigenetic modifications, are used to regulate transcription factor and polymerase access to transcriptional regulatory elements in chromatin. Epigenetic modification of chromatin permits the cells to retain acquired transcriptional regulation throughout cell division, providing a cellular identity to the progeny (12, 13). In addition, the development of distinct Th cell lineages has been shown to involve heritable epigenetic changes that regulate the expression of both lineage-specific transcription factors (including TBX21, RORC2, and GATA3) and cytokines (including IFN-γ, IL-17A, and IL-4) (14–16).

In this study, we examined the methylation patterns of regions of interest (ROI), identified by sequence homology analysis between

*Department of Experimental and Clinical Medicine, University of Florence, Florence 50134, Italy; [†]DENOTHE Center, University of Florence, Florence 50134, Italy; [‡]Department of Clinical and Experimental Medicine, Second University of Naples, Naples 80131, Italy; [§]Center for Biomolecular Studies Supporting Human Health, Second University of Naples, Naples 80131, Italy; [¶]Regenerative Medicine Unit, Careggi University Hospital, Florence 50134, Italy; [‖]Cell Biology Group, German Rheumatism Research Center Berlin, 10117 Berlin, Germany; [#]Regenerative Immunology and Aging, Berlin-Brandenburg Center for Regenerative Therapies, Charité University Medicine Berlin, 13353 Berlin, Germany; **Anna Meyer Children's Hospital and University of Florence, Florence 50134, Italy; and [††]Immunology and Cellular Therapy Unit, Careggi University Hospital, Florence 50134, Italy

[1]A.M. and V.S. contributed equally to this article.

[2]J.D. and F.A. share joint final authorship.

Received for publication May 20, 2014. Accepted for publication January 25, 2015.

This work was supported by grants from the Associazione Italiana per la Ricerca sul Cancro (Italy), Ministero dell'Istruzione, dell'Università e della Ricerca, the Italian Ministry of Health (RF-2010-2314610), the Ministero dell'Istruzione, dell'Università e della Ricerca, Progetti di Rilevante Interesse Nazionale 2009 (200999KRFW_003), and in part by the Bundesministerium für Bildung, Wissenschaft, Forschung und Technologie (S-T-THERA 01GU0802 to A.T. and A.R.; IMPAM 01EC1008B to A.R. and H.-D. C.), the Berlin-Brandenburg Center for Regenerative Therapies (1. Berlin-Brandenburg Center for Regenerative Therapies Grant to J.D. and A.T.), and the Deutsche Forschungsgemeinschaft (SFB 633 to A.T.; SFB 633 to A.R. and H.-D.C.).

Address correspondence and reprint requests to Prof. Francesco Annunziato, Department of Experimental and Clinical Medicine, University of Florence, Viale Pieraccini 6, Florence 50134, Italy. E-mail address: francesco.annunziato@unifi.it

Abbreviations used in this article: JIA, juvenile idiopathic arthritis; MNC, mononuclear cell; PB, peripheral blood; ROI, region of interest; ROR, retinoic acid orphan receptor; SF, synovial fluid; UCB, umbilical cord blood.

mice and humans, of the human genes *RORC2* (17), *TBX21, IL17A* (17), *IL17F* (18), and *IFNG* (19) in either human T cell clones or circulating freshly isolated $CD4^+$ T cells, isolated from both peripheral blood (PB) of healthy subjects and synovial fluid (SF) of juvenile idiopathic arthritis (JIA) patients, characterized by the following phenotypes: Th17, Th17/Th1, nonclassic (Th17-derived), and classic Th1. We further analyzed the methylation changes of the above-mentioned ROI in Th17 clones during the in vitro polarization of Th17 into the nonclassic Th1 phenotype. Our results demonstrate the existence of a strict relationship between Th17 and nonclassic Th1 cells, and support the concept that nonclassic and classic Th1 cells belong to two distinct cell lineages. These findings also identify the demethylated status of *RORC2* and *IL17A* ROI as useful markers of the "Th17 membership." Finally, the study of *RORC2* downstream ROI methylation status, as well as the PCR analysis at the single-cell level of the $CD4^+CD161^+$ T cell subset that contains all Th17 precursors (9), demonstrated the heterogeneity of this cell population, only partially composed of cells expressing *RORC2*, that is, potentially able to differentiate into Th17 cells. Altogether our data provide other important pieces in the puzzle of human Th17 cell physiology and heterogeneity.

Materials and Methods

Subjects

The PB samples were obtained from seven healthy donors. SF samples were collected from four JIA patients during routine therapeutic arthrocentesis. UCB samples were obtained from eight donors. The procedures followed in this study were in accordance with the ethical standards of the Regional Committee on Human Experimentation.

Reagents

The medium used was RPMI 1640 (Seromed, Berlin, Germany), supplemented with 2 mM L-glutamine, 1% nonessential amino acids, 1% pyruvate, 2 × 10-5 M 2-ME (Life Technologies Laboratories, Grand Island, NY), and 10% FCS (Euroclone). The following unlabeled or fluorochrome-conjugated mouse anti-human mAbs were used to stain cells: CD3, CD4, CD8, CD161, CCR6, CD45RA, CD45RO, CD31, IFN-γ, and isotype-matched control Abs (BD Biosciences, Mountain View, CA), IL-17A (eBioscience, San Diego, CA), and CD161 (Miltenyi Biotec, Bergisch Gladbach, Germany). PMA, ionomycin, brefeldin A, and saponin were from Sigma-Aldrich (St. Louis, MO). IL-1β, IL-6, IL-12, IL-23, and TGF-β were purchased from R&D Systems.

T cell recovery and expansion

Mononuclear cell (MNC) suspensions were obtained from PB, SF, and UCB by centrifugation on Ficoll-Hypaque gradient. PB $CD4^+$ T cells were negatively selected by high-gradient magnetic cell sorting (Miltenyi Biotec), as described by Cosmi et al. (9) and were then further divided into $CD161^+$ and $CD161^-$ by immunomagnetic cell sorting (Miltenyi Biotec). PB $CD4^+CD161^+$ and $CD4^+CD161^-$ T cell populations were further subdivided in $CCR6^+$ and $CCR6^-$ cell fractions by FACSAria (BD Biosciences) and then cultured under limiting dilution to obtain Th17 and Th1 clones, classified by flow cytometry for intracellular staining of IL-17A or IFN-γ cytokines (4). We stimulated in vitro four selected pure Th17 cell clones in the presence of allogeneic feeder cells, PHA (0.001% v/v) plus IL-2 (50 IU/ml), and the Th1-polarizing cytokine IL-12 (2 ng/ml). After 2 wk of in vitro activation, a significant proportion of cells started to produce IFN-γ. The Th17/Th1-polarized Th17 clones were then sorted by FACSAria into $CD4^+$IL-17A$^+$IFN-γ^-, $CD4^+$IL-17A$^+$IFN-γ^+, $CD4^+$IL-17A$^-$IFN-γ^+ T cell subpopulations, using the cytokine secretion assay, as described below. The $CD4^+$IL-17A$^-$IFN-γ^+ cell fraction of three of these polarized clones was then cultured again for 2 wk in the presence of IL-2 (50 IU/ml) alone, or with the addition of IL-1β (10 ng/ml) and IL-23 (20 ng/ml) or with IL-1β, IL-6 (2 ng/ml), IL-23, and TGF-β (5 ng/ml). PB $CD4^+$ naive T cells were obtained as $CD45RO^-CD45RA^+CD31^+$ by FACSAria. UCB $CD4^+$ T cells, negatively selected by high-gradient magnetic cell sorting (Miltenyi Biotec), were then pooled from eight samples and further divided into $CD161^+$ and $CD161^-$ T cell fractions by FACSAria. The same sorting strategy was followed to obtain $CD4^+CD161^+$ and $CD4^+CD161^-$ single cells from two independent UCB samples.

Cytokine secretion assay

PB and SF $CD4^+$ were negatively selected by high-gradient magnetic cell sorting and further divided into $CCR6^+$ and $CCR6^-$ cells by immunomagnetic cell sorting (Miltenyi Biotec), then were stained with anti-CD161 PE-Cy7, stimulated with PMA–ionomycin, recovered after 3.5 h, washed, and then stained with IFN-γ and IL-17A catch reagents (Miltenyi Biotec), according to the manufacturer's instructions. Following an additional 45 min of incubation (37°C, 5% CO_2), cells were stained with anti-CD3–Pacific Blue, -IL-17A–APC, and -IFN-γ–FITC; analyzed; and sorted by FACSAria. PB samples were divided into $CD4^+CCR6^+CD161^+$IL-17A$^+$IFN-γ^-, $CD4^+CCR6^+CD161^+$IL-17A$^+$IFN-γ^+, $CD4^+CCR6^+CD161^+$IL-17A$^-$IFN-γ^+, and $CD4^+CCR6^-CD161^-$IL-17A$^-$IFN-γ^+ T cell subsets, whereas SF samples were divided into $CD4^+CCR6^+CD161^+$IL-17A$^-$IFN-γ^+ and $CD4^+CCR6^-CD161^-$IL-17A$^-$IFN-γ^+ T cell subsets. Because of the low numbers of recovered cells, SF cell fractions were then expanded in vitro in the presence of IL-2 (50 IU/ml).

DNA methylation analysis

Genomic DNA was extracted and subsequently bisulfite was converted using the DNA Blood Mini Kit (QIAGEN, Hilden, Germany) and EZ DNA Methylation-Gold Kit (Zymo Research, Irvine, CA), respectively, according to the manufacturer's instructions. DNA methylation of the ROI was assessed by pyrosequencing of bisulfite-specific PCR products using standard procedures (Varionostic, Ulm, Germany), as described previously by Dong et al. (19). Briefly, 40 ng bisulfite-converted DNA was PCR amplified for the ROI of the IL17A, IL17F, IFNG, RORC2, and TBX21 genes using bisulfite-DNA–specific primers (Table I) in a PCR using the following program: 95°C for 3 min; 50 cycles of 95°C for 35 s, annealing temperature (Table I) for 35 s, and 72°C for 40 s; and a final extension at 72°C for 10 min. Bisulfite-PCR products were then subjected to pyrosequencing with the primers listed in Table I. Methylation levels at CpG sites were obtained using Pyro Q-CpG software.

RNA isolation, cDNA synthesis, and real-time quantitative RT-PCR

Total RNA was extracted using the RNeasy Micro Kit (QIAGEN) and treated with DNase I to eliminate possible genomic DNA contamination. TaqMan RT-PCR was performed as described by Santarlasci et al. (20). Primers and probes used were purchased from Life Technologies. Quantification was performed on cell number.

Single-cell real-time PCR

Single cells were sorted by FACSAria and then processed using a Single Cell to CT Kit (Life Technologies), according to the manufacturer's instructions. Briefly, single cells were lysed in the presence of DNase I prior to RNA reverse transcription. cDNA was then subjected to a preamplification step, using a panel of Taqman Gene Expression Assays (Life Technologies) of our interest. Preamplified cDNA was then quantitated by real-time PCR using Taqman Gene Expression Master Mix and Taqman Gene Expression Assays (Life Technologies) on a 7900HT Instrument (Life Technologies).

Statistics

The Mann–Whitney *U* test was used for DNA methylation analysis; the paired Student *t* test was used for mRNA expression analysis. A p value ≤ 0.05 was considered significant.

Results

Th17-derived (nonclassic) Th1 clones acquire demethylation at the IFNG and TBX21 but maintain hypomethylation at the RORC2 and IL17A

We have recently shown that human Th17 cells can be shifted in vitro into IFN-γ–producing cells (that we named as nonclassic Th1 cells) in the presence of IL-12 and/or TNF-α (4, 21, 22). We have also found increased numbers of nonclassic Th1 cells in the gut of patients with Crohn's disease, the skin of psoriatic patients, and the SF of patients suffering from JIA (9, 21, 23). Human nonclassic Th1 can be distinguished from classic Th1 cells because of the expression of Th17 cell–associated markers, such as CD161, CCR6, and RORC2 (10).

To define the epigenetic signatures of pure $CD4^+$ Th cell subsets, we decided to analyze DNA methylation of *TBX21, RORC2,*

Table I. Primer sequences

Target Region Primer	Sequence 5′–3′	Purpose	Annealing Temperature
IL-17A promoter F	TTTTTTTTTAGAAGGAGAGATT	Bisulfite PCR	
IL-17A promoter R	Biotin-TATTCCTAAATCTCCATAATC	Bisulfite PCR	52˚C
IL-17A promoter sequencing 1	AGGAGAGATTTTTTTATG	Pyrosequencing	
IL-17A promoter sequencing 2	AAGGAGAAAAGTTTTATAA	Pyrosequencing	
IL-17A promoter sequencing 3	TTATTGGTGGTGAGTT	Pyrosequencing	
IL-17F promoter F	GTGGTTTATTTTGTGTAGG	Bisulfite PCR	
IL-17F promoter R	Biotin-ATAAATTTTCTCCCATTTAA	Bisulfite PCR	52˚C
IL-17F promoter sequencing 1	GTATTTGTTAGTTTTATAGTAAT	Pyrosequencing	
IL-17F promoter sequencing 2	GTTTTTTTATAAATTGTTA	Pyrosequencing	
IFNg CNS-1 F	AGAAAAGGGGGGATTTA	Bisulfite PCR	
IFNg CNS-1 R	Biotin-TAACACTCACAACCAAATTATC	Bisulfite PCR	50˚C
IFNg CNS-1 sequencing 1	GGGGATTTAGAAAAAT	Pyrosequencing	
IFNg CNS-1 sequencing 2	TGTATGATGTTAGGAGTTT	Pyrosequencing	
IFNg promoter F	TGGTATAGGTGGGTATAAT	Bisulfite PCR	
IFNg promoter R	Biotin-TTACATATAAATCCTAACAATAAC	Bisulfite PCR	50˚C
IFNg promoter sequencing 1	TTATTTTAAAAAATTTGTG	Pyrosequencing	
IFNg promoter sequencing 2	TAATTTTTTTGGTTTAAT	Pyrosequencing	
Tbx21 F	TGGGAAATTAGTGGTTAT	Bisulfite PCR	
Tbx21R	Biotin-AAAAATCACCCCCTAT	Bisulfite PCR	52˚C
Tbx21 sequencing 1	GGGTTTATAGTATAGTTTTT	Pyrosequencing	
Tbx21 sequencing 2	TTTTATTTTAGGTTTATTTATA	Pyrosequencing	
RORC2 F	TATTGGGGGAGAGAGT	Bisulfite PCR	
RORC2 R	Biotin-AACATCCTCCTTTCCA	Bisulfite PCR	55˚C
RORC2 sequencing 1	GGAGAGAGTTAGGTGTAGA	Pyrosequencing	
RORC2 sequencing 2	TTGAGAAGGATAGGG	Pyrosequencing	

IFNG, IL17A, and *IL17F* gene loci (Table I), selected on the basis of evolutionary conservation among species and CpG site density in noncoding sequences (promoter and CNS) (24), in Th17, Th17/Th1, classic Th1, and nonclassic Th1 (Th17 derived), clones (Figs. 1, 2). As shown in Fig. 1A, we selected two ROI in the promoter of the *IL17A* and *IL17F* genes, respectively. The analysis of DNA methylation status of the two ROI by bisulfite pyrosequencing showed that Th17 and Th17/Th1 cells had a marked demethylation, and nonclassic Th1 cells exhibited a significant hypomethylation. In contrast, classic Th1 cells, as well as naive $CD4^+$ Th cells, were characterized by a complete methylation of the above-mentioned gene loci (Fig. 1A). As shown in Fig. 1B, two ROI in the *IFNG* gene locus were selected, the promoter and CNS-1 (located 4.2 kb upstream of the transcriptional start site) (19). The analysis of DNA methylation status of the two ROI by bisulfite pyrosequencing showed that whereas Th17/Th1, nonclassic Th1, and classic Th1 cells had a marked demethylation, Th17 cells and naive $CD4^+$ Th cells were characterized by a complete methylation (Fig. 1B). We also looked at the transcription factors involved in Th17 and Th1 development, and to this end, we analyzed one ROI for *RORC2* (*RORC2* downstream (17)) and one for *TBX21* (CNS-1). The analysis of DNA methylation status of the *RORC2* downstream showed that whereas Th17, Th17/Th1, and nonclassic Th1 cells had a marked demethylation, naive $CD4^+$ Th cells and classic Th1 cells were characterized by a complete methylation of this DNA region (Fig. 2A). Of interest, the analysis of DNA methylation status of the *TBX21* CNS-1 (Fig. 2B) showed that whereas nonclassic and classic Th1 cells had a marked demethylation, Th17 and Th17/Th1 cells were hypermethylated, compared with a complete methylation in naive $CD4^+$ Th cells. These findings strongly support the concept that nonclassic Th1 cells originate from Th17 cells.

To provide additional evidence for this possibility, we decided to stimulate in vitro four Th17 clones in the presence of allogeneic feeder cells and IL-12. As expected on the basis of the results of our previous study (4), after 2 wk of activation, a significant proportion of clonal cells started to produce IFN-γ (Fig. 3). $IL\text{-}17A^+IFN\text{-}\gamma^-$, $IL\text{-}17A^+IFN\text{-}\gamma^+$, and $IL\text{-}17A^-IFN\text{-}\gamma^+$ cell fractions were then obtained by cell sorting, and DNA methylation of *TBX21, RORC2, IFNG, IL17A,* and *IL17F* gene loci was analyzed. As indicated in Fig. 3B and 3D, all three cell fractions showed, independently of their ability to produce IL-17A, complete demethylation of *IL17A* and *RORC2,* and hypomethylation of *IL17F* ROI, demonstrating an epigenetic imprinting of Th17 origin in these cells. Of note, only IFN-γ–producing cell subsets ($IL\text{-}17A^+IFN\text{-}\gamma^+$ and $IL\text{-}17A^-IFN\text{-}\gamma^+$ cells) were characterized by a significant hypomethylation of the *IFNG* promoter, when compared with cells producing IL-17A alone (Fig. 3C). Moreover, all three cell subsets also showed complete demethylation of the ROI in *TBX21* (Fig. 3E).

To understand whether the acquisition of the nonclassic Th1 phenotype by Th17 cells was only a transient or a stable phenomenon, $IL\text{-}17A^-IFN\text{-}\gamma^+$ cell fractions were FACS sorted from in vitro polarized Th17 clones and then cultured for an additional 2 wk under neutral (medium alone) or Th17-polarizing (IL-1β plus IL-23 or IL-1β plus IL-6 plus IL-23 plus TGF-β) conditions. Irrespective of the different culture conditions, the totality of the cells was able to produce IFN-γ, as assessed at the single-cell level upon PMA plus ionomycin stimulation (data not shown). Accordingly, as shown in Fig. 3F, methylation analysis of the IFNG promoter and CNS-1 of cells cultured under Th17 polarizing conditions clearly showed stability of the demethylated status.

RORC2 is methylated in classic, but hypomethylated in nonclassic, ex vivo Th1 cells derived from both normal and inflamed tissues

To confirm these findings obtained on T cell clones, we extended our analysis in different ex vivo $CD4^+$ Th subsets isolated from PB by separation procedures based on both the expression of surface markers and the ability of cells to produce different cytokines. Th17 cells were obtained as $CD4^+CD161^+CCR6^+IL\text{-}17A^+IFN\text{-}\gamma^-$, Th17/Th1 cells as $CD4^+CD161^+CCR6^+IL\text{-}17A^+IFN\text{-}\gamma^+$, nonclassic Th1 cells as $CD4^+CD161^+CCR6^+IL\text{-}17A^-IFN\text{-}\gamma^+$, and classic Th1 cells as $CD4^+CD161^-CCR6^-IL\text{-}17A^-IFN\text{-}\gamma^+$ cells (Fig. 4A). Because of the paucity of circulating $CD4^+CD161^+$ T cells, and to avoid a possible modulation of the Th cell phenotype owing to in vitro expansion, the above-mentioned cell populations were

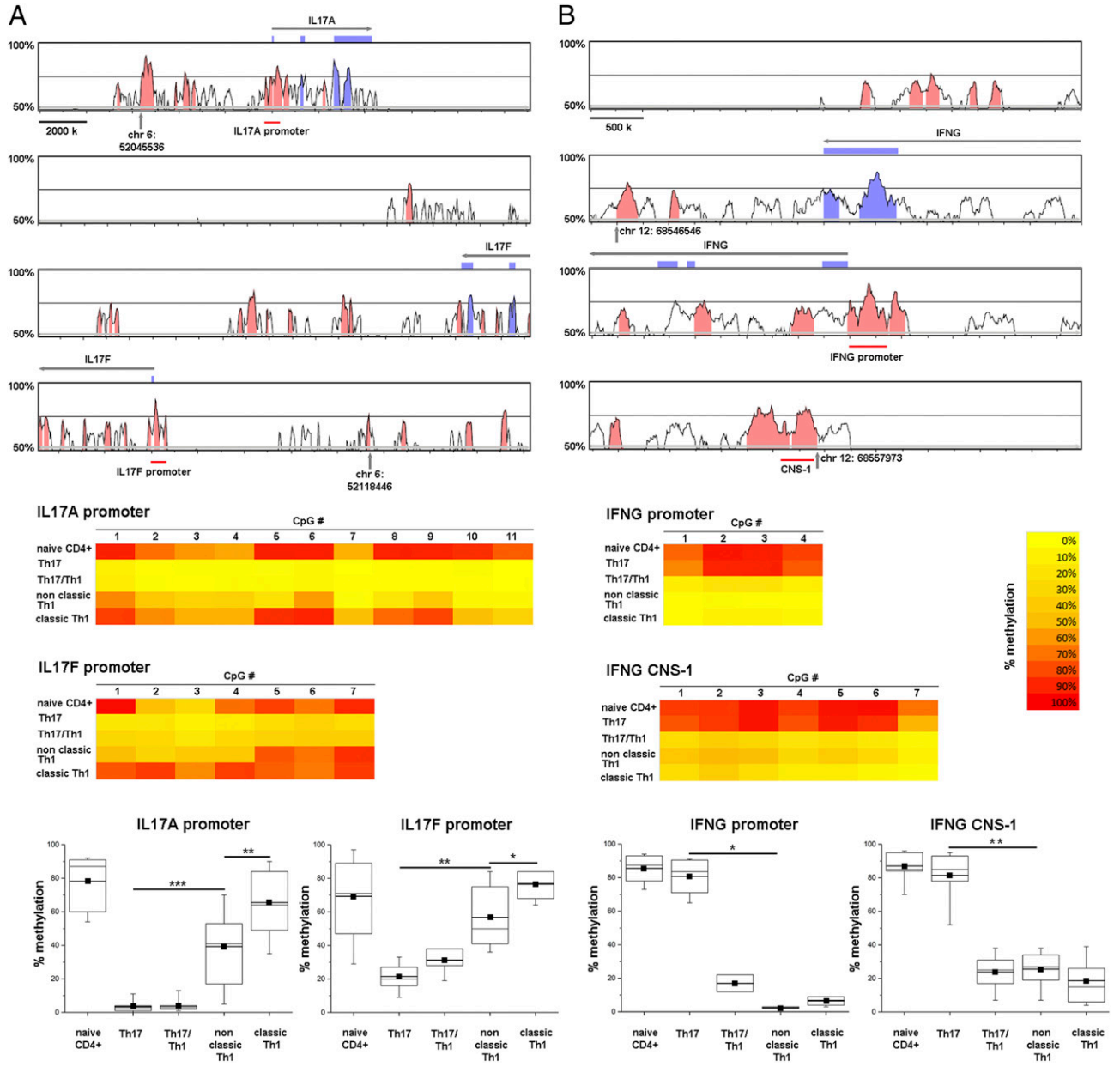

FIGURE 1. DNA methylation analysis of *IL17A, IL17F,* and *IFNG* gene loci in T cell clones with different Th phenotypes. Alignment of human and mouse genomes at *IL17A*, *IL17F* (**A**), and *IFNG* (**B**) gene loci was performed using Vista software (30). DNA sequence identity >50% (*y*-axis) over ≥100 bp is indicated in the histogram plot. Arrows indicate transcription direction. Pink regions indicate conserved noncoding sequences, whereas blue regions are conserved coding sequences (*top of each panel*). DNA methylation status of PB $CD4^+$ naive T cells and of Th17, Th17/Th1, nonclassic, and classic Th1 clones are represented as colorimetric-code (yellow-red scale). Methylation level at each CpG site is the average of three T cell clones for each subset (*middle of each panel*). The distribution of the average methylation levels at each CpG site of the whole region is depicted also as a box plot for each population. Medians and 25th and 75th percentiles are shown in boxes, lines with filled square represent the means, and minimum and maximum values are shown as whiskers (*bottom of each panel*).*$p \leq 0.05$, **$p \leq 0.01$, ***$p \leq 0.001$.

collected from pooled buffy coats of five individual donors. To verify the quality of cell sorting, the ex vivo–derived Th17, Th17/Th1, nonclassic, and classic Th1 cell fractions were then analyzed for *RORC2*, *TBX21*, *IL17A*, and *IFNG* mRNA expression. As shown in Fig. 4B, ex vivo–derived Th17 and Th17/Th1 cells expressed high *RORC2* and *IL17A*, but low *IFNG*, as well as intermediate *TBX21* mRNA levels, whereas classic Th1 cells were characterized by high *TBX21* and *IFNG*, but low *RORC2* and *IL17A*, mRNA levels. In contrast to classic Th1 cells, nonclassic Th1 cells exhibited intermediate *RORC2* mRNA levels (Fig. 4B). Next, we analyzed DNA methylation of *TBX21, RORC2, IFNG, IL17A,* and *IL17F* gene loci in these ex vivo Th17, Th17/Th1, classic, and nonclassic Th1 cell fractions. As shown in Fig. 4, ex vivo Th17 cells exhibited a complete demethylation of the *RORC2* (Fig. 4E) and *IL17A* (Fig. 4C) ROI, and hypomethylation of the *IL17F* (Fig. 4C) and *TBX21* (Fig. 4F) ROI, but hypermethylation of the *IFNG* (Fig. 4D) ROI, when compared with $CD4^+$ naive Th cells. Ex vivo Th17/Th1 cells were characterized by hypomethylation of all the *RORC2, IL17A*, *IL17F*, *TBX21,* and *IFNG* ROI, when compared with $CD4^+$ naive Th cells (Fig. 4C–F), in line with their mixed phenotype. Strikingly, in contrast to classic Th1 cells, nonclassic Th1 cells were characterized by significant hypomethylation of both *RORC2* (Fig. 4E) and *IL17A* ROI (Fig. 4C). In contrast, *IFNG* and *TBX21* ROI were almost equally demethylated on both nonclassic and classic Th1 cells (Fig. 4D, 4F), whereas *IL17F* ROI was hypermethylated on both nonclassic and classic Th1 cells (Fig. 4C).

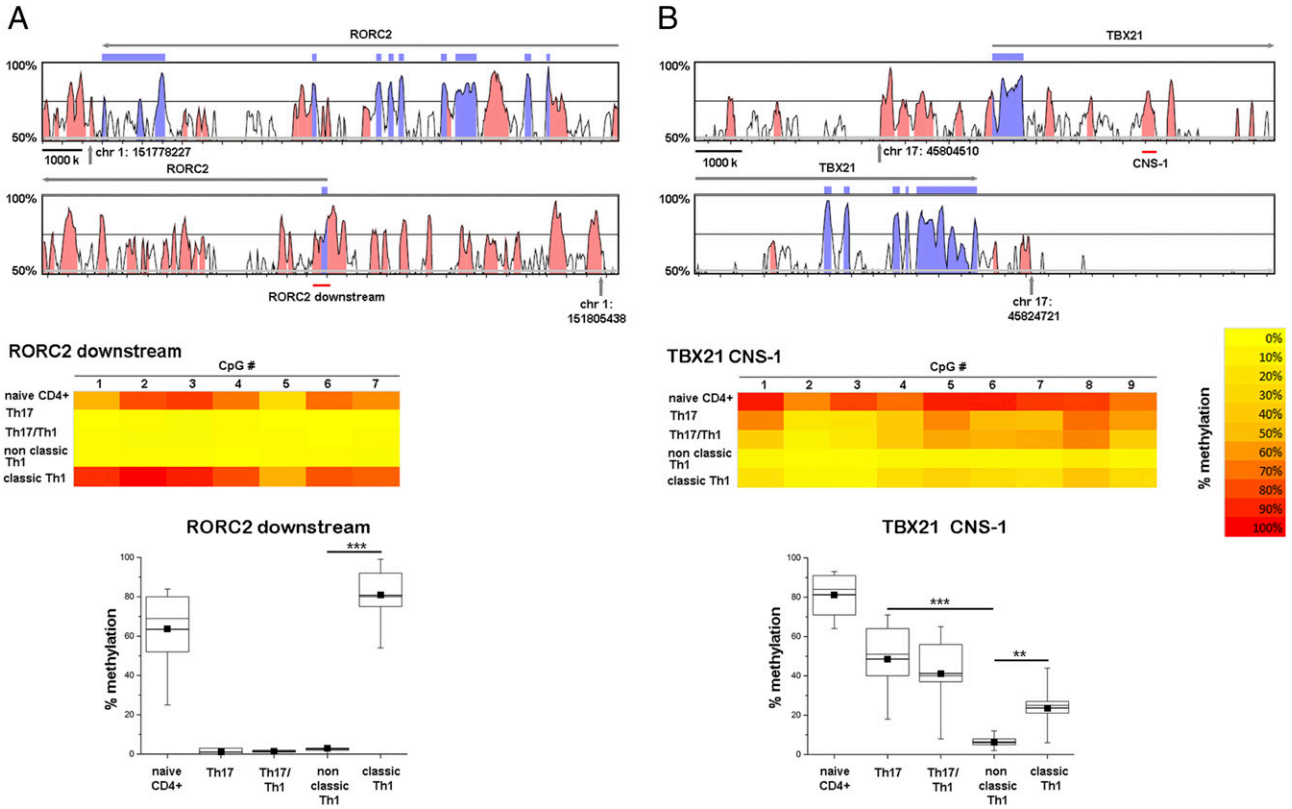

FIGURE 2. DNA methylation analysis of *RORC2* and *TBX21* gene loci in T cell clones with different Th phenotype. Alignment of human and mouse genomes at *RORC2* (**A**) and *TBX21* (**B**) gene loci was performed as described in Fig. 1. DNA methylation status of PB $CD4^+$ naive T cells and of Th17, Th17/Th1, nonclassic, and classic Th1 clones are represented as colorimetric-code (yellow-red scale). Methylation level at each CpG site is the average of three T cell clones for each subset (*middle of each panel*). The distribution of the average methylation levels at each CpG site of the whole region is depicted also as a box plot for each population. Medians and 25th and 75th percentiles are shown in boxes, lines with filled square represent the means, and minimum and maximum values are shown as whiskers (*bottom of each panel*). $^{**}p \leq 0.01$, $^{***}p \leq 0.001$.

To assess the methylation status of nonclassic and classic Th1 cells in diseased patients, we isolated $CD4^+CD161^+CCR6^+IL\text{-}17A^-IFN\text{-}\gamma^+$ (nonclassic Th1) cells and $CD4^+CD161^-CCR6^-IL\text{-}17A^-IFN\text{-}\gamma^+$ (classic Th1) cells from the SF of four JIA patients. Unfortunately, the number of cells was insufficient to make direct methylation analysis. For this reason, we performed quantitative PCR analysis of *TBX21, RORC2, IL17A,* and *IFNG* on all ex vivo isolated classic and nonclassic Th1 cells. Moreover, we analyzed DNA methylation of *TBX21, RORC2, IFNG, IL17A,* and *IL17F* gene loci on in vitro expanded classic and nonclassic Th1 cells derived from two of the four JIA patients. As shown in Fig. 5A, ex vivo nonclassic Th1 cells expressed higher *IL17A* and *RORC2* (with the latter reaching statistical significance) but equal *IFNG* and *TBX21* mRNA levels, when compared with classic Th1 cells. Accordingly, as shown in Fig. 5, 2-wk in vitro expanded nonclassic Th1 cells exhibited reduced methylation of the *RORC2* (Fig. 5D), *IL17A,* and *IL17F* promoters (Fig. 5B) and *IFNG* CNS-1 (Fig. 5C) ROI, when compared with classic Th1 cells. No differences in the methylation of *IFNG* promoter (Fig. 5C) and *TBX21* CNS-1(Fig. 5F) ROI were appreciable between nonclassic and classic Th1 cells (Fig. 5).

Only a minority of human naive $CD4^+CD161^+$ cells represent Th17 precursors

In a previous study, we showed that human Th17 cells originate from a small population of $CD4^+CD161^+$ Th cell precursors present in both UCB and newborn thymus (9). This small population of naive $CD4^+CD161^+$ T cells exhibited high *RORC2*, *IL23R*, *CCR6*, and *IL1R1* mRNA levels, whereas the much more abundant $CD4^+CD161^-$ naive Th cell counterpart virtually did not. However, the $CD4^+CD161^+$ naive Th cells were unable to produce IL-17A, unless they were activated in vitro in the presence of IL-23 and IL-1β, whereas the $CD4^+CD161^-$ naive Th cells could never be induced to produce IL-17A (9). On the basis of these findings, we decided to analyze DNA methylation of the *RORC2* gene locus in these two populations as a tool to better define the nature of human Th17 precursors. To this end, ex vivo UCB-derived $CD4^+CD161^+$ and $CD4^+CD161^-$ T cell fractions were separated by cell sorting and first analyzed for *RORC2* mRNA expression. As expected, ex vivo–derived UCB-derived $CD4^+CD161^+$ cells expressed high *RORC2* mRNA levels, whereas *RORC2* mRNA levels in UCB-derived $CD4^+CD161^-$ cells were virtually undetectable (Fig. 6A). Surprisingly, however, *RORC2* ROI was hypermethylated similarly in both $CD4^+CD161^+$ and $CD4^+CD161^-$ UCB-derived populations (Fig. 6B).

To explain this apparent contradiction, we hypothesized that only a small minority of the whole population of $CD4^+CD161^+$ naive Th cells was expressing *RORC2*. To provide experimental support for this hypothesis, we performed PCR analysis of *RORC2*, *IL23R*, *IL1R1,* and on ex vivo UCB-derived $CD4^+CD161^+$ and $CD4^+CD161^-$ cells even at the single-cell level.

This approach was used because bisulfite analysis cannot be performed on single cells; however, it is reasonable to speculate that the detection on a single cell of a given mRNA can be considered a sign of permissive methylation status of the gene locus in the same cell. Therefore, single-cell PCR analysis was performed on a total number of 100 cells from ex vivo UCB-derived $CD4^+$

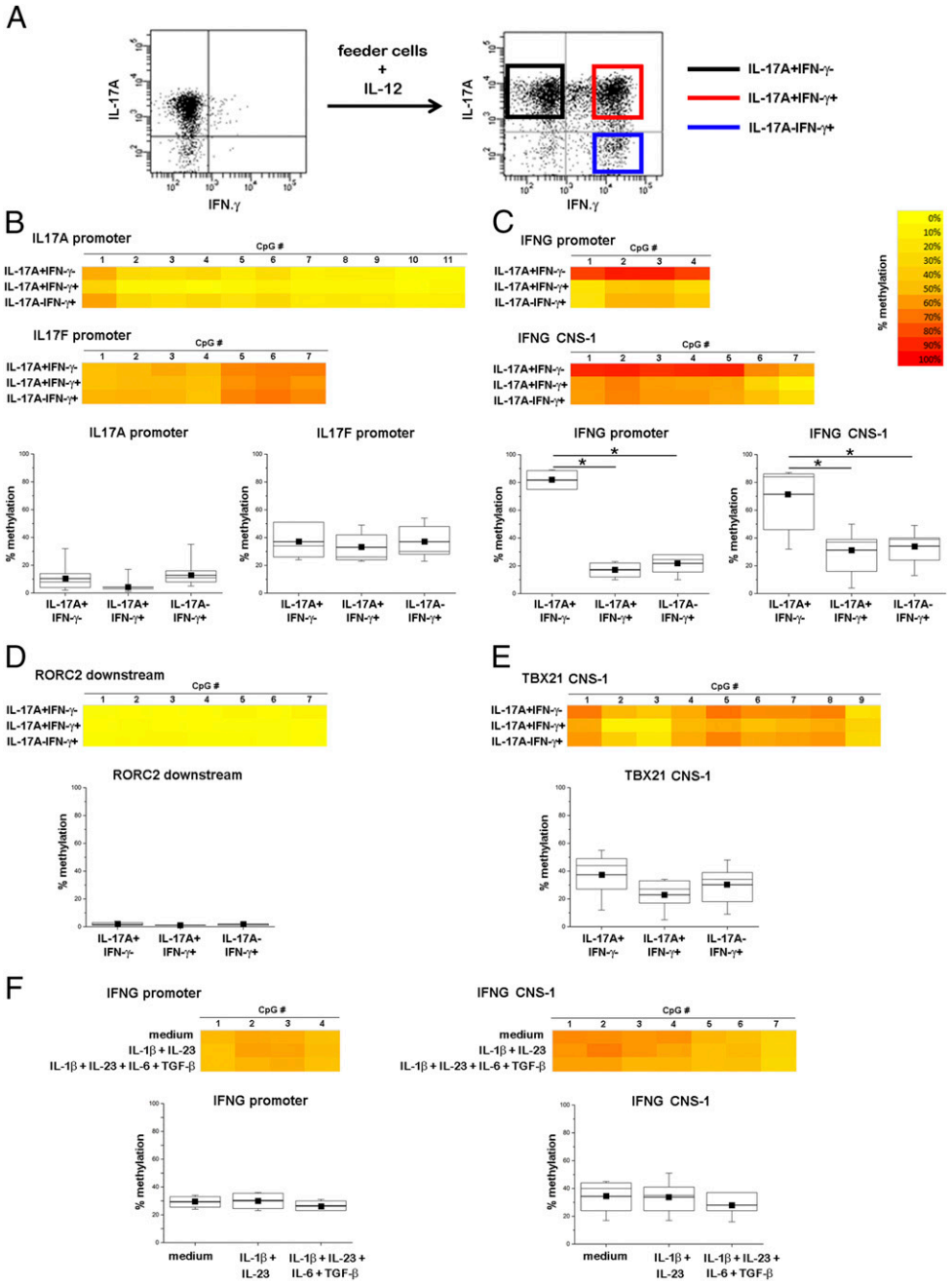

FIGURE 3. Demethylation of the *IFNG* promoter accompanies Th17 polarization toward the Th17/Th1 phenotype. Four selected pure Th17 cell clones were polarized in vitro toward Th1 by culturing in the presence of allogeneic feeder cells and the pro-Th1 cytokine IL-12 for 2 wk. (**A**) Cytokine production was evaluated by intracellular staining after PMA plus ionomycin stimulation before and after polarization. On day 15, cells were sorted on the basis of their cytokine profile. The IL-17A$^-$IFN-γ$^+$ fraction of three of the above-mentioned Th1-polarized Th17 clones was then cultured in medium alone or in Th17-favoring conditions (IL-1β and IL-23 or IL-1β, IL-6, IL-23, and TGF-β) for 2 additional weeks. DNA methylation status at *IL17A* and *IL17F* (**B**), *IFNG* (**C** and **F**), *RORC2* (**D**), and *TBX21* (**E**) genes in the indicated cell subsets or culture conditions was represented as colorimetric-code (yellow-red scale). Methylation level at each CpG site is the average of three or four T cell clones for each subset (*middle of each panel*). The distribution of the average methylation levels at each CpG site of the whole region is depicted also as a box plot for each population. Medians and 25th and 75th percentiles are shown in boxes, lines with filled square represent the means, and minimum and maximum values are shown as whiskers (*bottom of each panel*). *$p \leq 0.05$.

CD161$^+$ and CD4$^+$CD161$^-$ cells (50 cells for each cell subset from two different donors). Data obtained on UCB bulk cells subsets confirmed our previous observations (9, 11), that is, that *RORC2*, *IL23R*, *CCR6,* and *IL1R1* mRNA was highly expressed on CD4$^+$CD161$^+$ compared with CD4$^+$CD161$^-$ cell fractions (Fig. 6C). Moreover, single-cell PCR analysis revealed that only a fraction of CD4$^+$CD161$^+$ cells expressed the analyzed mRNA and indicated a frequency of *RORC2*-expressing cells of 25% (CB1 = 18%, CB2 = 32%) in the CD4$^+$CD161$^+$ cell fraction and of 0% (CB1 = 0%, CB2 = 0%) in the CD4$^+$CD161$^-$ counterpart (Fig. 6D and data not shown). In addition, 5% (CB1 = 4%, CB2 = 6%) of the CD4$^+$CD161$^+$ cells analyzed expressed *IL23R* and none of them expressed *IL1R1* and *CCR6* (Fig. 6D and data not shown). None of the CD4$^+$CD161$^-$ T cells expressed *IL23R*, *IL1R1*, or *CCR6* (Fig. 6D and data not shown). Of note, all the few cells expressing *IL23R* were contained in the *RORC2*-positive cell fraction (Fig. 7).

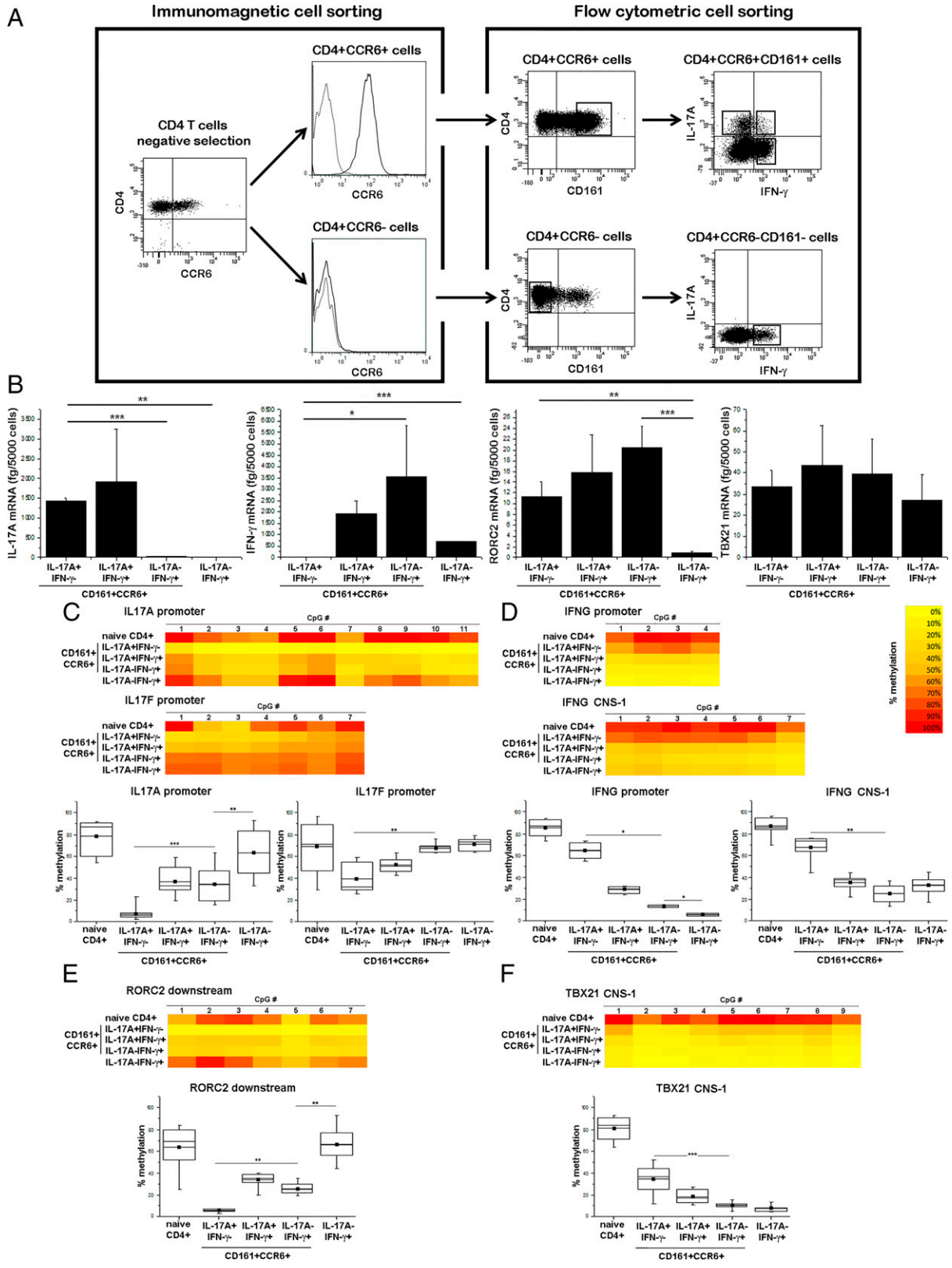

FIGURE 4. Ex vivo–derived cytokine-producing Th cells exhibit the same DNA methylation status of T cell clones. (**A**) Sorting strategy for the isolation of $CD4^+CCR6^+CD161^+IL\text{-}17A^+IFN\text{-}\gamma^-$, $CD4^+CCR6^+CD161^+IL\text{-}17A^+IFN\text{-}\gamma^+$, $CD4^+CCR6^+CD161^+IL\text{-}17A^-IFN\text{-}\gamma^+$, $CD4^+CCR6^-CD161^-IL\text{-}17A^-IFN\text{-}\gamma^+$ T cell populations from PB MNC. One of five is depicted. $CD4^+$ cells were negatively selected from PB MNC and then further divided into $CCR6^+$ and $CCR6^-$ populations by MACS sorting. Afterward, these populations were stimulated with PMA plus ionomycin to perform secretion assay, and were sorted by FACS based on IFN-γ, IL-17A, and CD161 expression. (**B**) Real-time quantitative PCR analysis of *IL17A*, *IFNG*, *RORC2*, and *TBX21* mRNA levels. Columns represent means ± SE of mRNA fg/5000 cells of the different T cell populations from five healthy donors. DNA methylation status at *IL17A* and *IL17F* (**C**), *IFNG* (**D**), *RORC2* (**E**), *TBX21* (**F**) genes in PB $CD4^+$ naive T cells and in the ex vivo–derived Th cell subsets pooled from five donors, was represented as colorimetric code (yellow-red scale, *top of the panel*). DNA methylation levels of the whole region are depicted also as a box plot for each population. Medians and 25th and 75th percentiles are shown in (*Figure legend continues*)

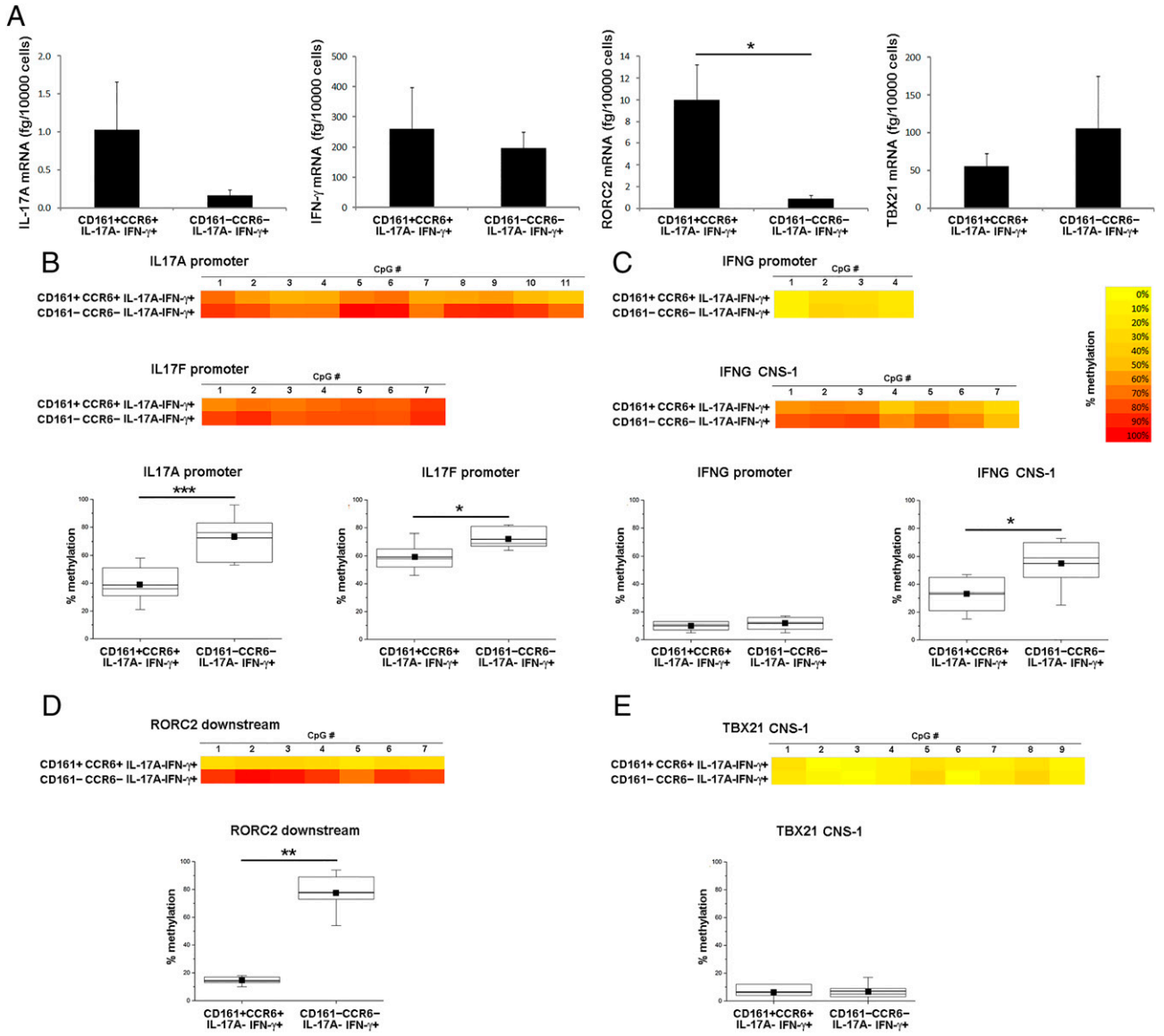

FIGURE 5. In vitro expanded SF-derived nonclassic Th1 cells display demethylation of *RORC2* and *IL17A* gene loci. (**A**) Real-time quantitative PCR analysis of the *IL17A*, *IFNG*, *RORC2*, and *TBX21* mRNA levels from SF-derived nonclassic and classic Th1 cells. $CD4^+$ cells were negatively selected from SF and then further divided into $CCR6^+$ and $CCR6^-$ populations by MACS sorting. Afterward, these populations were stimulated with PMA plus ionomycin to perform secretion assay, and were sorted by FACS based on IFN-γ, IL-17A, and CD161 expression. Columns represent means ± SE of mRNA fg/10,000 cells of the two T cell populations from four JIA patients. DNA methylation status at *IL17A* and *IL17F* (**B**), *IFNG* (**C**), *RORC2* (**D**), and *TBX21* (**E**) genes in in vitro expanded SF-derived Th1 cell subsets pooled from two patients, was represented as colorimetric code (yellow-red scale, *top of the panel*). DNA methylation levels of the whole region are depicted also as a box plot for each population. Medians and 25th and 75th percentiles are shown in boxes, lines with filled square represent the means, and minimum and maximum values are shown as whiskers (*bottom of each panel*). $*p \leq 0.05$, $**p \leq 0.01$, $***p \leq 0.001$.

Discussion

For many years, in both murine experimental models and human diseases, Th1 cells have been thought to be responsible for chronic inflammation and organ-specific autoimmune disorders (25). However, this scenario has been completely changed by the recent discovery, first in mice and then in humans, of a new lineage of $CD4^+$ T helper cells that produce IL-17A and express the transcription factor RORγt (RORC2 in humans), named Th17 (3). Several models of knockout mice provided evidence that supports the pathogenicity of Th17 cells, whereas Th1 cells were considered to be mainly protective at the sites of inflammation (26–28). A possible answer to this question can come from the observation that Th17 and Th1 phenotypes are not mutually exclusive. Studies performed in our laboratory demonstrated first that a portion of human IL-17A–secreting cells are also able to simultaneously produce IFN-γ (Th17/Th1 cells) and provided evidence that both Th17 and Th17/Th1 cells can be shifted to the production of IFN-γ alone (named as nonclassic Th1 cells) (4, 10). Following these initial findings in humans, the Th17 cell plasticity was demonstrated even in mice (29).

boxes, lines with filled square represent the means, and minimum and maximum values are shown as whiskers (*bottom of each panel*). $*p \leq 0.05$, $**p \leq 0.01$, $***p \leq 0.001$.

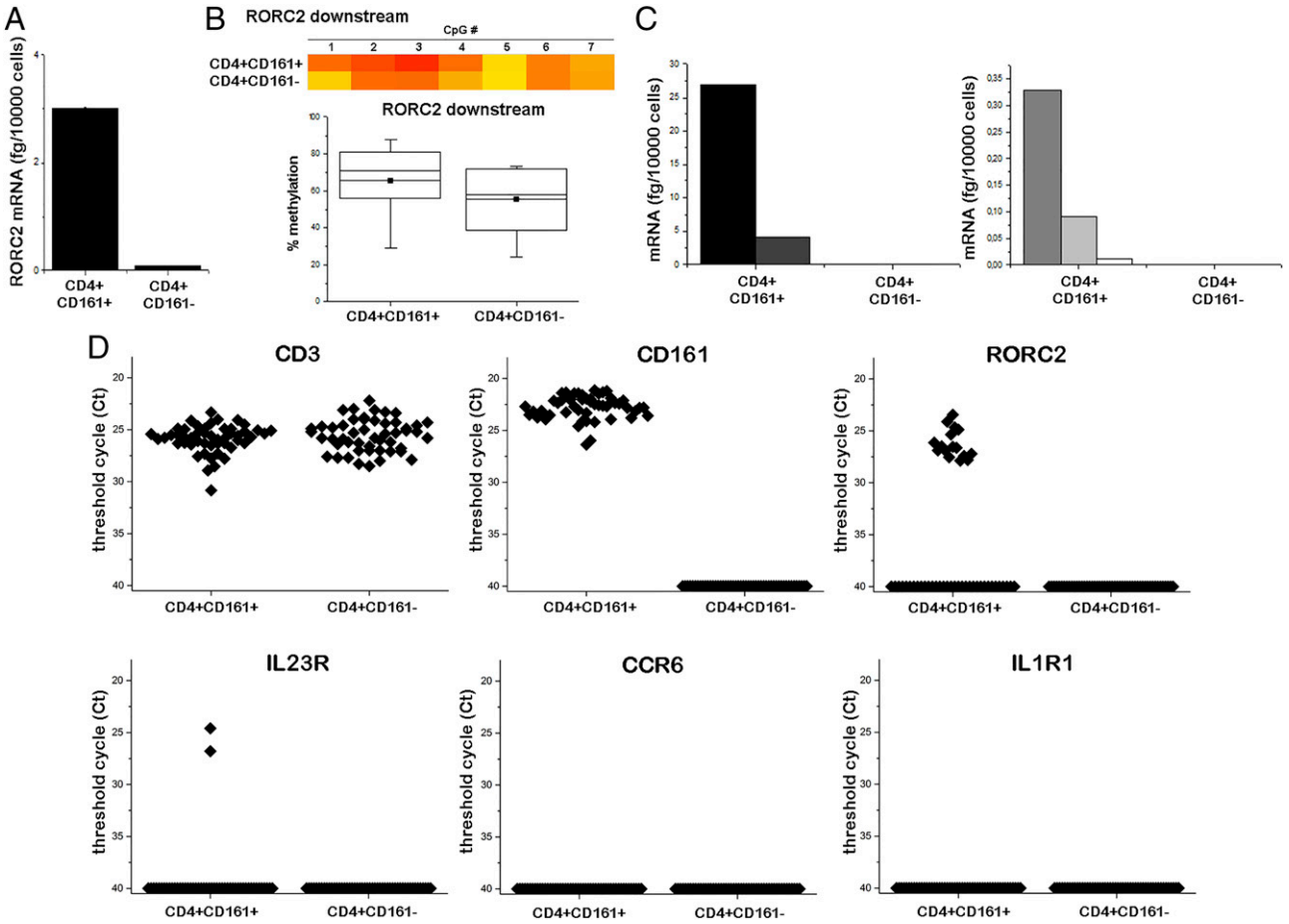

FIGURE 6. *RORC2* is expressed by a small fraction of $CD4^+CD161^+$ naive T cells. (**A**) Real-time quantitative PCR analysis of the mRNA levels of *RORC2* in $CD4^+CD161^+$ and $CD4^+CD161^-$ cells pooled from eight UCB samples. Columns represent means of three replicates of mRNA levels. (**B**) DNA methylation status at *RORC2* gene in $CD4^+CD161^+$ and $CD4^+CD161^-$ UCB cells pooled from eight donors was represented as colorimetric-code (yellow-red scale; see previous figures). The distribution of the average methylation levels at each CpG site of the whole region is depicted also as a box plot for each population. Medians and 25th and 75th percentiles are shown in boxes, lines with filled square represent the means, and minimum and maximum values are shown as whiskers (*bottom of each panel*). (**C**) Real-time quantitative PCR analysis of the mRNA levels of *CD161* (black column), *RORC2* (dark gray column), *IL23R* (gray column), *CCR6* (light gray column), and *IL1R1* (white column) in $CD4^+CD161^+$ and $CD4^+CD161^-$ cells was represented. One of two different UCB analyzed is depicted. Columns represent means of three replicates of mRNA levels. (**D**) Single-cell real-time quantitative PCR of the mRNA levels of *CD3ε*, *CD161*, *RORC2*, *IL23R*, *CCR6*, and *IL1R1* in $CD4^+CD161^+$ and $CD4^+CD161^-$ cells in one of two UCB analyses performed. Each cell is represented as a diamond. Data are indicated as Ct values.

Despite the findings that support the Th17 origin of nonclassic Th1 cells, it was recently shown that in vitro expanded human Th1 and Th17 cells, as well as intermediate Th17/Th1 cells, have distinct epigenetic signatures at cytokine (*IFNG* and *IL17A*) and transcription factor *RORC2,* but not at transcription factor *TBX21*, gene loci (17). The results of this study were based on the isolation of different $CD4^+$ Th subsets from PB, thanks to the development of a flow cytometry–based method that took advantage of the different expressions of CCR6, CD161, and CXCR3. $CCR6^+CD161^+$ $CXCR3^-$ $CD4^+$ T cells were defined as Th17 cells, $CCR6^+$ $CXCR3^+$ cells as Th17/Th1 cells, and $CCR6^-CXCR3^+$ as Th1 cells (17). However, the Th17/Th1 cells, as defined by applying the Cohen (17) flow cytometry–based method, indeed represented a mixed population, containing not only cells producing both IL-17A and IFN-γ but also Th17-derived (nonclassic) Th1 cells. In addition, owing to the low numbers of cells collected from a single donor, the different cell fractions required in vitro expansions in the presence of autologous feeder cells for 2 wk, thus possibly causing undesired effects of cell polarization and/or modulation.

To identify a more convincing epigenetic signature of pure Th17, Th17/Th1, classic, and nonclassic Th1 cells, we decided to evaluate DNA methylation levels at cytokine (*IFNG*, *IL17A*, and *IL17F*) and transcription factor (*TBX21* and *RORC2*) gene loci of the above-mentioned Th cell subsets obtained from four different sources: 1) Th17, Th17/Th1, classic, and nonclassic Th1 clones; 2) $IL\text{-}17A^+$ $IFN\text{-}\gamma^-$ (Th17), $IL\text{-}17A^+IFN\text{-}\gamma^+$ (Th17/Th1), and $IL\text{-}17A^-IFN\text{-}\gamma^+$ (nonclassic Th1) cells derived from the in vitro polarization of a Th17 cell clone; 3) PB MNC ex vivo isolated $CD4^+CCR6^+CD161^+$ $IL\text{-}17A^+IFN\text{-}\gamma^-$ (Th17) cells, $CD4^+CCR6^+CD161^+IL\text{-}17A^+IFN\text{-}\gamma^+$ (Th17/Th1) cells, $CD4^+CCR6^+CD161^+IL\text{-}17A^-IFN\text{-}\gamma^+$ (nonclassic Th1) cells, and $CD4^+CCR6^-CD161^-IL\text{-}17A^-IFN\text{-}\gamma^+$ (classic Th1) cells; and 4) in vitro expanded $CD4^+CCR6^+CD161^+IL\text{-}17A^-IFN\text{-}\gamma^+$ (nonclassic Th1) and $CD4^+CCR6^-CD161^-IL\text{-}17A^-IFN\text{-}\gamma^+$ (classic Th1) cells derived from the SF of JIA patients. The data clearly demonstrate that Th17 cells, in agreement with their mRNA expression profile, were characterized by low methylation levels at *RORC2*, *IL17A*, and *IL17F*, and by high methylation levels at *IFNG,* gene loci. In accordance with their mixed phenotype, in addition to hypomethylation of *RORC2*, *IL17A*, and *IL17F* gene loci, Th17/Th1 cells showed higher demethylation levels of *TBX21* and *IFNG* gene loci when compared with Th17 cells. Of note, nonclassic Th1, derived from both PBMC of healthy subjects and SF of JIA-affected

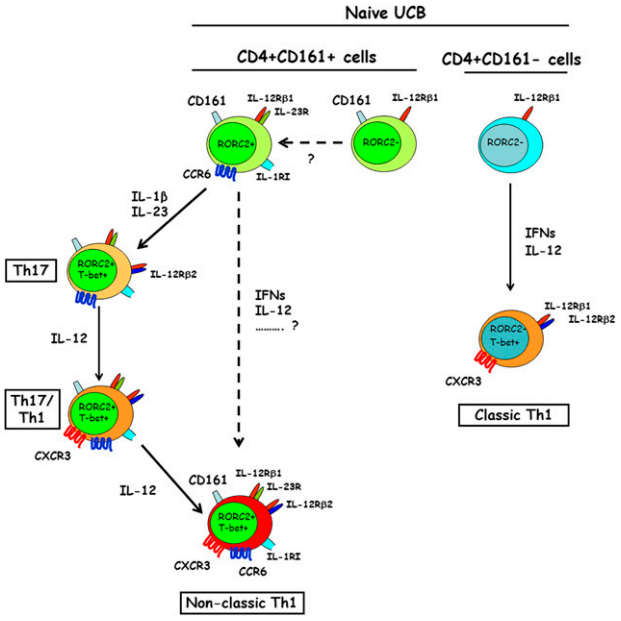

FIGURE 7. Schematic representation of nonclassic and classic Th1 cell development. Developmental stages of UCB $CD4^+CD161^+$ and $CD4^+CD161^-$ cell differentiation toward nonclassic and classic Th1 phenotypes, respectively, are represented. Continuous arrows indicate differentiation stages; dotted arrows suggest hypothesized and unknown maturation processes. Among the UCB $CD4^+CD161^+$ cell fraction, $RORC2^+$ cells first develop into Th17 but then can be rapidly shifted toward the nonclassic Th1 subset under the activity of IL-12 signals. It is actually unknown whether the Th17 step is mandatory for the final acquisition of the nonclassic Th1 status or whether UCB $CD4^+CD161^+RORC2^+$ cells can be immediately directed toward this phenotype. UCB $CD4^+CD161^+RORC2^-$ cells may represent an immature population, which can acquire RORC2 expression upon proper stimulation. UCB $CD4^+CD161^-RORC2^-$ cells instead directly acquire a classic Th1 phenotype when in the presence of appropriate stimuli.

patients, could be distinguished from classic Th1 cells not only because of the demethylation of the *RORC2* gene locus but also because of their lower methylation levels at the *IL17A* gene promoter. Finally, and in support of the data obtained on purified Th cell subsets, we found that the IFN-γ–secreting cell fractions derived from the in vitro polarization of Th17 clones were characterized by progressive *IFNG* promoter demethylation, whereas the *RORC2* gene locus and *IL17A* promoter maintained a complete demethylated status. More importantly, we demonstrated that the acquired *IFNG* promoter demethylation was maintained after 2 wk of in vitro cultures of the IFN-γ–producing cell fraction in the presence of Th17-polarizing cytokines.

Taken together, these data clearly establish at the molecular level the existence of a strict relationship between Th17 and nonclassic Th1 cells, supporting the concept that nonclassic and classic Th1 cells belong to two distinct cell lineages. Obviously, it cannot be excluded that the activation of naive UCB Th17 precursors ($CD4^+CD161^+$ T cells) in the presence of Th1-polarizing conditions may induce a direct polarization of these cells toward the Th1 phenotype (Fig. 7). These findings also identify the demethylated status of *RORC2* and *IL17A* ROI as useful stable epigenetic markers of the "Th17 membership," in addition to the expression of CD161 and CCR6 (8). Increased numbers of nonclassic Th1 cells have been found in patients with JIA or Crohn's disease (21, 23), suggesting that acquisition of the ability to produce IFN-γ by Th17 cells occurs in vivo and associates with chronic inflammatory responses. It seems likely that nonclassic Th1 cells can play a pivotal role in the establishment and persistence of the disease because their number at the level of the inflammatory sites directly correlates with parameters of disease activity (21). Therefore, further examination of the epigenetic profile of Th1 cells from patients with chronic inflammatory disorders will be key to a better understanding of their origin. This issue is also very important from a practical point of view because the knowledge of whether these cells are primarily pathogenic mediators or have protective functions will help to identify which cell types should be therapeutically targeted in a variety of diseases.

In this study, we also investigated the DNA methylation signature at the *RORC2* locus in human Th17 cell precursors, which are known to be contained within the $CD4^+CD161^+$ population of UCB cells (9). This population displays *RORC2*, *IL23R*, *CCR6*, and *IL1R1* gene expression, whereas its $CD161^-$ counterpart virtually does not. Therefore, we assessed DNA methylation levels at the *RORC2* promoter in $CD4^+CD161^+$ and $CD4^+CD161^-$ UCB cells. Unexpectedly, comparable methylation levels between these two cell sources were found, allowing us to hypothesize that Th17 cell precursors expressing *RORC2* are only a small fraction of the entire $CD4^+CD161^+$ UCB population. Therefore, owing to the impossibility of performing bisulfite sequencing on single cells, we performed single-cell real-time PCR on $CD4^+CD161^+$ and $CD4^+CD161^-$ UCB cells. In agreement with our hypothesis, we found that only 25% of the $CD4^+CD161^+$ cells and none of the $CD4^+CD161^-$ cells exhibited *RORC2* mRNA. Accordingly, only 20% of clones expressing *RORC2* mRNA could be obtained by culturing single $CD4^+CD161^+$ naive T cells in the presence of IL-1β and IL-23 (data not shown). The analysis of *IL23R*, *CCR6,* and *IL1R1* mRNA levels on single cells showed that they were expressed by none of the $CD161^-$ cells, whereas only 5% of the $CD161^+$ cells expressed *IL23R*. Of note, all these *IL23R*-positive cells were expressing *RORC2*. Although we were able to detect *CCR6* and *IL1R1* mRNA expression on the $CD161^+$ bulk population, we found no single cells expressing them, thus suggesting a frequency of positive cells $<1\%$. These data identify one more "tile in the puzzle" of Th17 cell physiology. Taken together, they confirm that only $CD4^+CD161^+$, but not $CD4^+CD161^-$, naive Th cells contain *RORC2*-expressing Th17 precursors and demonstrate that these latter cells represent only a minority of the entire $CD4^+CD161^+$ T cell population. This finding explains why in our previous studies (9, 11) we were unable to polarize the entire UCB-derived $CD4^+CD161^+$ cells toward the Th17 phenotype following their in vitro activation in the presence of IL-1β plus IL-23. This small subset of $CD4^+CD161^+$*RORC2*$^+$ cells may express IL-23R, and perhaps also CCR6 and IL-1R1, probably in later phases of their development, whereas they acquire the ability to produce IL-17A only following exposure to IL-1β and IL-23 in the tissue environment. However, currently we cannot exclude the possibility that the $CD4^+CD161^+RORC2^-$ cells represent a still immature stage, which, under certain microenviromental conditions, may be induced to acquire the RORC2 expression (Fig. 7).

Acknowledgments

We thank M.K. Levings for providing *RORC2* downstream sequence and primers.

Disclosures

The authors have no financial conflicts of interest.

References

1. Mosmann, T. R., and R. L. Coffman. 1989. TH1 and TH2 cells: different patterns of lymphokine secretion lead to different functional properties. *Annu. Rev. Immunol.* 7: 145–173.

2. Romagnani, S. 1994. Lymphokine production by human T cells in disease states. *Annu. Rev. Immunol.* 12: 227–257.
3. Harrington, L. E., R. D. Hatton, P. R. Mangan, H. Turner, T. L. Murphy, K. M. Murphy, and C. T. Weaver. 2005. Interleukin 17-producing CD4+ effector T cells develop via a lineage distinct from the T helper type 1 and 2 lineages. *Nat. Immunol.* 6: 1123–1132.
4. Annunziato, F., L. Cosmi, V. Santarlasci, L. Maggi, F. Liotta, B. Mazzinghi, E. Parente, L. Filì, S. Ferri, F. Frosali, et al. 2007. Phenotypic and functional features of human Th17 cells. *J. Exp. Med.* 204: 1849–1861.
5. Lee, Y. K., H. Turner, C. L. Maynard, J. R. Oliver, D. Chen, C. O. Elson, and C. T. Weaver. 2009. Late developmental plasticity in the T helper 17 lineage. *Immunity* 30: 92–107.
6. Hirota, K., J. H. Duarte, M. Veldhoen, E. Hornsby, Y. Li, D. J. Cua, H. Ahlfors, C. Wilhelm, M. Tolaini, U. Menzel, et al. 2011. Fate mapping of IL-17-producing T cells in inflammatory responses. *Nat. Immunol.* 12: 255–263.
7. Lexberg, M. H., A. Taubner, I. Albrecht, I. Lepenies, A. Richter, T. Kamradt, A. Radbruch, and H. D. Chang. 2010. IFN-γ and IL-12 synergize to convert in vivo generated Th17 into Th1/Th17 cells. *Eur. J. Immunol.* 40: 3017–3027.
8. Annunziato, F., L. Cosmi, F. Liotta, E. Maggi, and S. Romagnani. 2012. Defining the human T helper 17 cell phenotype. *Trends Immunol.* 33: 505–512.
9. Cosmi, L., R. De Palma, V. Santarlasci, L. Maggi, M. Capone, F. Frosali, G. Rodolico, V. Querci, G. Abbate, R. Angeli, et al. 2008. Human interleukin 17-producing cells originate from a CD161+CD4+ T cell precursor. *J. Exp. Med.* 205: 1903–1916.
10. Maggi, L., V. Santarlasci, M. Capone, M. C. Rossi, V. Querci, A. Mazzoni, R. Cimaz, R. De Palma, F. Liotta, E. Maggi, et al. 2012. Distinctive features of classic and nonclassic (Th17 derived) human Th1 cells. *Eur. J. Immunol.* 42: 3180–3188.
11. Maggi, L., V. Santarlasci, M. Capone, A. Peired, F. Frosali, S. Q. Crome, V. Querci, M. Fambrini, F. Liotta, M. K. Levings, et al. 2010. CD161 is a marker of all human IL-17-producing T-cell subsets and is induced by RORC. *Eur. J. Immunol.* 40: 2174–2181.
12. Riggs, A. D., V. E. A. Russo, and R. A. Martienssen. 1996. *Epigenetic mechanisms of gene regulation.* Cold Spring Harbor Laboratory Press, Cold Spring Harbor, N.Y.
13. Bird, A. 2007. Perceptions of epigenetics. *Nature* 447: 396–398.
14. Janson, P. C., L. B. Linton, E. A. Bergman, P. Marits, M. Eberhardson, F. Piehl, V. Malmström, and O. Winqvist. 2011. Profiling of CD4+ T cells with epigenetic immune lineage analysis. *J. Immunol.* 186: 92–102.
15. Wei, G., L. Wei, J. Zhu, C. Zang, J. Hu-Li, Z. Yao, K. Cui, Y. Kanno, T. Y. Roh, W. T. Watford, et al. 2009. Global mapping of H3K4me3 and H3K27me3 reveals specificity and plasticity in lineage fate determination of differentiating CD4+ T cells. *Immunity* 30: 155–167.
16. Wilson, C. B., E. Rowell, and M. Sekimata. 2009. Epigenetic control of T-helper-cell differentiation. *Nat. Rev. Immunol.* 9: 91–105.
17. Cohen, C. J., S. Q. Crome, K. G. MacDonald, E. L. Dai, D. L. Mager, and M. K. Levings. 2011. Human Th1 and Th17 cells exhibit epigenetic stability at signature cytokine and transcription factor loci. *J. Immunol.* 187: 5615–5626.
18. Hedrich, C. M., T. Rauen, K. Kis-Toth, V. C. Kyttaris, and G. C. Tsokos. 2012. cAMP-responsive element modulator α (CREMα) suppresses IL-17F protein expression in T lymphocytes from patients with systemic lupus erythematosus (SLE). *J. Biol. Chem.* 287: 4715–4725.
19. Dong, J., H. D. Chang, C. Ivascu, Y. Qian, S. Rezai, A. Okhrimenko, L. Cosmi, L. Maggi, F. Eckhardt, P. Wu, et al. 2013. Loss of methylation at the IFNG promoter and CNS-1 is associated with the development of functional IFN-γ memory in human CD4(+) T lymphocytes. *Eur. J. Immunol.* 43: 793–804.
20. Santarlasci, V., L. Maggi, M. Capone, V. Querci, L. Beltrame, D. Cavalieri, E. D'Aiuto, R. Cimaz, A. Nebbioso, F. Liotta, et al. 2012. Rarity of human T helper 17 cells is due to retinoic acid orphan receptor-dependent mechanisms that limit their expansion. *Immunity* 36: 201–214.
21. Cosmi, L., R. Cimaz, L. Maggi, V. Santarlasci, M. Capone, F. Borriello, F. Frosali, V. Querci, G. Simonini, G. Barra, et al. 2011. Evidence of the transient nature of the Th17 phenotype of CD4+CD161+ T cells in the synovial fluid of patients with juvenile idiopathic arthritis. *Arthritis Rheum.* 63: 2504–2515.
22. Maggi, L., R. Cimaz, M. Capone, V. Santarlasci, V. Querci, G. Simonini, F. Nencini, F. Liotta, S. Romagnani, E. Maggi, et al. 2014. Brief report: etanercept inhibits the tumor necrosis factor α-driven shift of Th17 lymphocytes toward a nonclassic Th1 phenotype in juvenile idiopathic arthritis. *Arthritis Rheum. (Munch)* 66: 1372–1377.
23. Maggi, L., M. Capone, F. Giudici, V. Santarlasci, V. Querci, F. Liotta, F. Ficari, E. Maggi, F. Tonelli, F. Annunziato, and L. Cosmi. 2013. CD4+CD161+ T lymphocytes infiltrate Crohn's disease-associated perianal fistulas and are reduced by anti-TNF-α local therapy. *Int. Arch. Allergy Immunol.* 161: 81–86.
24. Dong, J., C. Ivascu, H. D. Chang, P. Wu, R. Angeli, L. Maggi, F. Eckhardt, L. Tykocinski, C. Haefliger, B. Möwes, et al. 2007. IL-10 is excluded from the functional cytokine memory of human CD4+ memory T lymphocytes. *J. Immunol.* 179: 2389–2396.
25. Gately, M. K., L. M. Renzetti, J. Magram, A. S. Stern, L. Adorini, U. Gubler, and D. H. Presky. 1998. The interleukin-12/interleukin-12-receptor system: role in normal and pathologic immune responses. *Annu. Rev. Immunol.* 16: 495–521.
26. Cua, D. J., J. Sherlock, Y. Chen, C. A. Murphy, B. Joyce, B. Seymour, L. Lucian, W. To, S. Kwan, T. Churakova, et al. 2003. Interleukin-23 rather than interleukin-12 is the critical cytokine for autoimmune inflammation of the brain. *Nature* 421: 744–748.
27. Murphy, C. A., C. L. Langrish, Y. Chen, W. Blumenschein, T. McClanahan, R. A. Kastelein, J. D. Sedgwick, and D. J. Cua. 2003. Divergent pro- and antiinflammatory roles for IL-23 and IL-12 in joint autoimmune inflammation. *J. Exp. Med.* 198: 1951–1957.
28. Iwakura, Y., and H. Ishigame. 2006. The IL-23/IL-17 axis in inflammation. *J. Clin. Invest.* 116: 1218–1222.
29. Murphy, K. M., and B. Stockinger. 2010. Effector T cell plasticity: flexibility in the face of changing circumstances. *Nat. Immunol.* 11: 674–680.
30. Frazer, K. A., L. Pachter, A. Poliakov, E. M. Rubin, and I. Dubchak. 2004. VISTA: computational tools for comparative genomics. *Nucleic Acids Res.* 32: W273–279.